minerals

MDPI

Article

CFD Modeling and Cold Physical Model Simulation on Single Molten Slag Ligament Disintegration into Droplets

Ming Zhao, Yuhua Pan *, Aifu Zhao, Shili Zhang, Ping Ma and Xin Feng

School of Materials and Metallurgy, University of Science and Technology Liaoning, Anshan 114051, China
* Correspondence: 320153200140@ustl.edu.cn

Abstract: Aiming at the mode of liquid ligament disintegration into droplets in the process of the centrifugal granulation of molten blast furnace slag using a spinning cup, in order to gain an in-depth understanding of the behavior and mechanism of droplet formation by liquid ligament disintegration and to obtain appropriate conditions to control the size of the produced slag granules, a three-dimensional CFD model describing water–air two-phase flow with a free surface was established in this work for simulating the process of a single water ligament breakup into droplets under the action of gravity, surface tension and inertial forces, so as to compare with the process of a molten slag ligament disintegration into droplets due to centrifugal force exerted by the spinning cup. By studying the disintegration behavior and mechanism of a single water ligament, the similar phenomenon of a molten slag ligament disintegration is examined. The numerical simulation results on the breakup of a single water ligament show that the length of the ligament before its disintegration and the diameter of the droplets formed both increase with the increase of the velocity of the ligament initially exiting a capillary nozzle. In addition, an experimental set-up was established in the laboratory to conduct cold physical model simulation experiments on single water or liquid paraffin ligament disintegration. The experimental results are compared with the numerical simulation results so that the reliability of the CFD model is verified. The results of the present study show that, in the centrifugal granulation process of blast furnace slag using a spinning cup operated in the ligament disintegration mode, the breakup of a single molten slag ligament is very similar to that of a single water or liquid paraffin ligament, and both approximately follow the Rayleigh Disintegration Mechanism, which provides a theoretical basis for analyzing the breakup process of the ligaments of different liquids as references for guiding the operation of centrifugal granulation of molten slag.

Keywords: centrifugal granulation of molten slag; liquid ligament; droplet; CFD numerical simulation; cold physical model simulation; Rayleigh Disintegration Mechanism

Citation: Zhao, M.; Pan, Y.; Zhao, A.; Zhang, S.; Ma, P.; Feng, X. CFD Modeling and Cold Physical Model Simulation on Single Molten Slag Ligament Disintegration into Droplets. *Minerals* **2023**, *13*, 139. https://doi.org/10.3390/min13020139

Academic Editor: Sharif Jahanshahi

Received: 6 December 2022
Revised: 8 January 2023
Accepted: 16 January 2023
Published: 18 January 2023

1. Introduction

The technology of spinning cup granulation of molten blast furnace slag has nowadays become a worldwide research hotspot [1] due to its high processing capacity (60 t/h~360 t/h) [2], high heat recovery rate, strong adaptability, simple equipment design, minimal water consumption, limited pollution on the environment and high quality of granulated slag particles with potentially higher value-added applications. In the spinning cup granulation process, the starting temperature of molten blast furnace slag must be higher than about 1400 °C to ensure the slag fluidity. However, at high temperatures, the slag cools slowly due to its low thermal conductivity and, thus, the slag heat is released slowly, which has an adverse impact on the amount of glass content created. Therefore, the best way to resolve this paradox is to reduce the size of the slag particles generated by granulation [3]. The particle diameter is the main basis for the evaluation of the process efficiency and offers the direction for setting operating conditions [4]. The particle size and its distribution are significantly impacted by the mode of slag film breakup in the centrifugal granulation process with spinning cups. More specifically, the liquid ligament breakup mode in the

centrifugal granulation process under certain appropriate operating conditions is thought to be the optimal granulation mode since this granulation mode produces fine slag granules with more uniform size distribution than other granulation methods can provide [5].

Studies [6] have shown that when the blast furnace slag is granulated in the mode of liquid ligament breakup, the diameter of each ligament of molten slag broken into droplets is generally consistent with that theoretically predicted following the Rayleigh Disintegration Mechanism [7]. To verify this, in the present work CFD numerical model simulations and cold physical model experimental simulations were conducted on the process of a single water ligament breakup into droplets driven by gravity and surface tension forces. To investigate the influence of liquid viscosity, the process of a single liquid paraffin ligament breakup into droplets was also studied using the cold physical model. Both the mathematical and physical simulation results were compared with the process of liquid slag ligament breakup into droplets driven by centrifugal and surface tension forces during spinning cup granulation of molten blast furnace slag and with the correlation derived from the Rayleigh Disintegration Mechanism.

In the present work, the reason for focusing on the breakup process of a water ligament instead of a molten slag ligament was the consideration of easy experimentation, because it is very hard to establish high-temperature experiments on molten slag ligament breakup, but rather easier to facilitate such experiments using water at room temperature. Another reason is the fact that, regardless of the type of liquid, when the liquid ligament becomes thin enough, the surface tension force will eventually dominate the breakup process, so that the liquid ligament will follow the Rayleigh Disintegration Mechanism to break into droplets. Therefore, it is logical and generally reasonable to start with simulation on water ligament breakup and use the water modeling results to validate the CFD model to be developed. Then, the CFD model will be applied to simulate the ligament breakup processes of different liquids including water, liquid paraffin and molten slag.

It is hoped that the results of this work will offer a theoretical foundation for the advancement of spinning cup granulation technology for the treatment of blast furnace slag and guide the direction for the technology's scale-up and realization of practical applications.

2. Model Development

2.1. CFD Model Description

The process of a water ligament breakup into droplets, driven by gravity and surface tension forces, is a typical free surface flow phenomenon. There is a distinct interface (i.e., free surface) between the fluid phases in the process, which involves both the gas phase (air) and the liquid phase (water). The present work suggests the following general assumptions to simplify the numerical simulations on the above-mentioned multiphase flow process:

(1) Unsteady-state incompressible fluid flow;
(2) Contant fluid physical properties;
(3) Axially symmetrical flow about the liquid ligament centerline.

Based on the above assumptions, a three-dimensional unsteady-state CFD model of water–air two-phase flow was established to simulate the disintegration of a water ligament under the influence of surface tension, gravity and inertial forces. Figure 1 schematically shows the computation domain and mesh defined for the CFD model.

The computational domain is defined as a 30° angle sector of vertical cylinder that is initially filled with air, meaning that the volume fraction of gas phase in the domain is one, whereas the volume fraction of liquid phase is zero. The top, side and bottom faces of the computational domain are set as openings where the air can enter or leave the computational domain and water droplets are allowed to leave the bottom face. The inlet of the water ligament is located at top face center, where its centerline is coincident with the center axis of the cylindrical computation domain, which is set as the symmetrical axis. To reduce the computational amount, the computation domain only covers a fraction (1/12) of the cylinder that is bounded by two vertical planes, which intersect at the center axis and form a 30° angle (θ) with each other. These two planes are defined as symmetrical

planes. As boundary conditions, zero fluxes of all the variables are applied to both the center axis and the symmetrical planes. Water enters the computational domain at a certain velocity at the ligament inlet. Table 1 lists the detail boundary conditions defined for the CFD model, and Table 2 provides the relevant physical properties of water and air used in the simulation work.

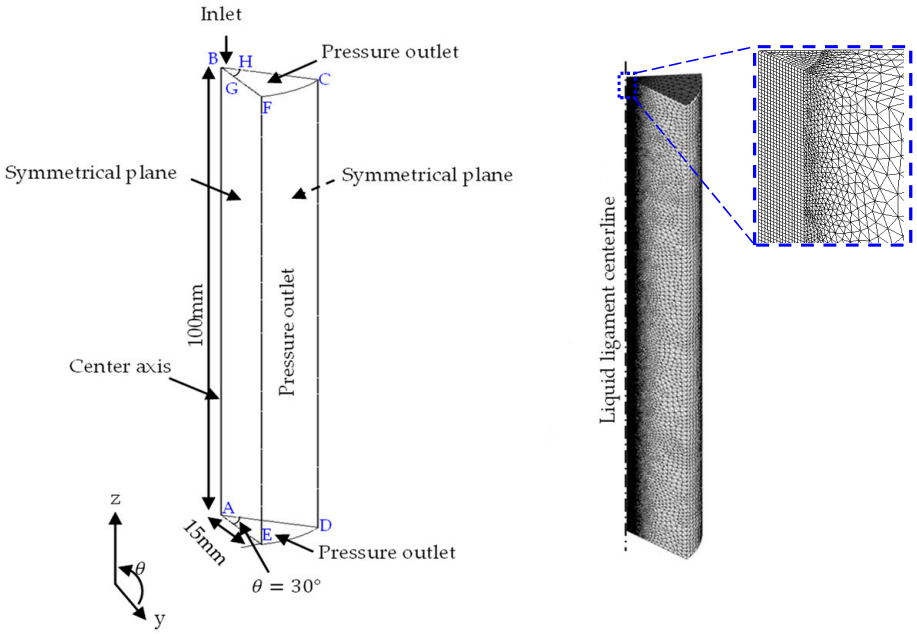

(**a**) Computation domain (**b**) Computation mesh

Figure 1. Schematic illustration of computation domain and mesh defined for CFD model.

Table 1. Boundary conditions defined for CFD model.

Boundary Name	Location	Type	Condition
Inlet	BGH	Inlet	Constant flow rate
Bottom face	ADE	Pressure outlet	Constant pressure
Top face	BCF	Pressure outlet	Constant pressure
Side face 1	CDEF	Pressure outlet	Constant pressure
Side face 2	ABCD	Symmetrical plane	Zero flux
Side face 3	ABFE	Symmetrical plane	Zero flux
Ligament centerline	AB	Symmetrical axis	Zero flux

Table 2. Physical properties of air and water at 25 °C used in CFD model [8].

Material	Density ($kg \cdot m^{-3}$)	Dynamic Viscosity ($Pa \cdot s$)	Surface Tension ($N \cdot m^{-1}$)
Air	1.185	1.831×10^{-5}	-
Water	997	0.0009	0.073

As indicated by the enlarged inset of Figure 1b, there is a hybrid computation mesh comprising both structured and unstructured grids in different (inner and outer) regions of the computation domain. The structured grids are defined mainly in the inner region where the liquid ligament breaks into droplets. These grids (with typical lengths smaller than 0.0001 m) are small enough for numerically resolving the droplets generated. In the outer region of the computation domain away from the ligament breakup zone to limit the computation amount, relative larger grids (with a maximum length of 0.0015 m) are defined that are unstructured so as to make a smooth transition between the fine grids in the inner region and the coarse grids in the outer region.

In order to check the sensitivity of the simulation results to the grid size, three different sizes of the structured grids in the inner region of the computation domain are set in a range from 0.00005 m to 0.0001 m, thus generating 807,841, 1,205,222 and 1,564,006 grids, respectively. Because the mesh size in the inner region, where the ligament breaks into droplets, is the most important for numerically resolving the droplets (i.e., the droplet-air interface), CFD models with these three numbers of grids were first executed under the same conditions. A comparison among the simulation results, in terms of liquid volume fraction variation along the radial direction of a water droplet at similar position and time, for the three sets of computation mesh are shown in Figure 2. It can be seen from this figure that as the number of grids increases the slope of liquid volume fraction variation along the radial distance becomes larger, meaning that the droplet-air interface is numerically resolved better. Furthermore, the liquid volume fraction distribution for the grid number of 1,205,222 is very close to that for the grid number of 1,564,006, whereas that for the grid number of 807,841 is relatively farther away. Thus, for the sake of saving computation amount, a computation mesh with 1,205,222 grids would be sufficient for accuracy and, thus, was used in the present CFD model for all the subsequent investigations.

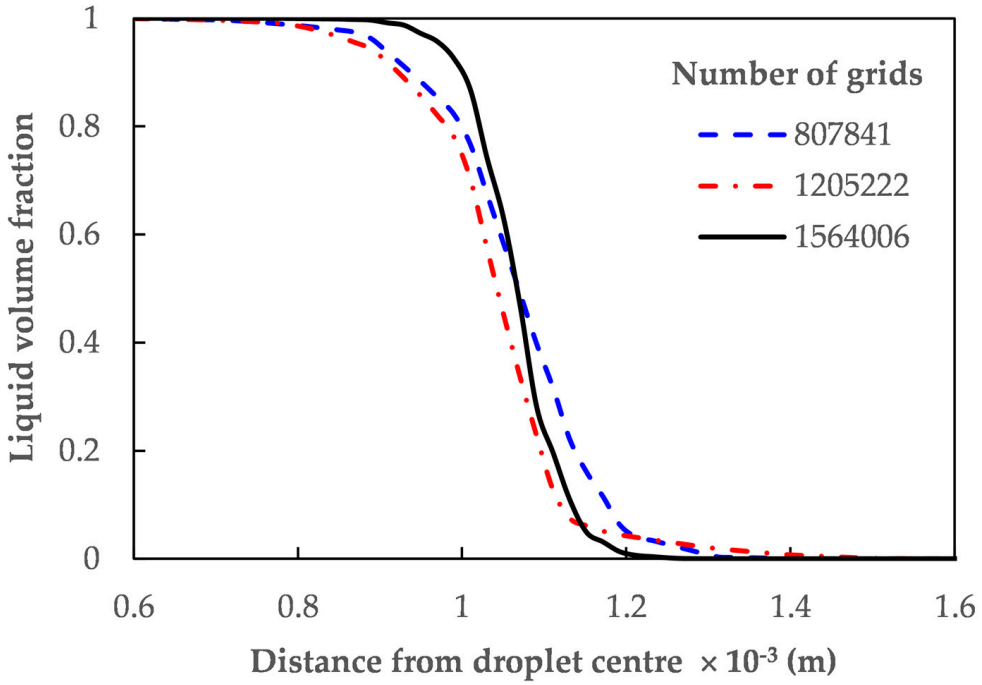

Figure 2. Comparison in liquid volume fraction variation along droplet radial direction predicted using present CFD model with different numbers of computation grids.

2.2. Governing Equations

Based on the aforementioned general assumptions, the turbulent multiphase flows involving the breakup of a water ligament into droplets are numerically simulated using a volume of fluid (VOF) method [9] together with turbulence effect modeled by using the Shear Stress Transport (SST) approach, which can be described by the following partial differential equations:

(1) Continuity equation:

$$\frac{\partial \rho}{\partial t} + \nabla \cdot (\rho \boldsymbol{u}) = 0 \tag{1}$$

(2) Momentum transport equations:

$$\begin{gathered} \frac{\partial (\rho \boldsymbol{u})}{\partial t} + \nabla \cdot (\rho \boldsymbol{u}\boldsymbol{u}) = \\ -\nabla p + \nabla \cdot [(\mu + \mu_t)(\nabla \boldsymbol{u} + (\nabla \boldsymbol{u})^T)] + F_g + F_s \end{gathered} \tag{2}$$

(3) SST turbulence equations:

$$\frac{\partial(\rho k)}{\partial t} + \nabla\cdot(\rho \boldsymbol{u} k) = \nabla\cdot[(\mu + \frac{\mu_t}{\sigma_{k3}})\nabla k] + P_k - \beta'\rho k\omega \tag{3}$$

$$\begin{gathered}\frac{\partial(\rho\omega)}{\partial t} + \nabla\cdot(\rho \boldsymbol{u}\omega) = \\ \nabla\cdot[(\mu + \frac{\mu_t}{\sigma_{\omega 3}})\nabla\omega] + (1 - F_1)2\rho\frac{\nabla k\nabla\omega}{\sigma_{\omega 2}\omega} + \alpha_3\frac{\omega}{k}P_k - \beta_3\rho\omega^2\end{gathered} \tag{4}$$

(4) Volume fraction equations:

$$\frac{\partial r_\alpha}{\partial t} + \nabla\cdot(r_\alpha \boldsymbol{u}_\alpha) = 0 \tag{5}$$

$$\sum_{\alpha=1}^{N_p} r_\alpha = 1 \tag{6}$$

where, ρ is the density (kg·m^{-3}); $\boldsymbol{u}$ is the velocity vector (m·s^{-1}); p is the pressure (Pa); μ is the dynamic viscosity (Pa·s); μ_t is the turbulent viscosity (Pa·s); F_g is the source term due to gravity (N·m^{-3}); F_s is the source term due to surface tension force (N·m^{-3}), which is calculated using the Continuum Surface Force (CSF) method of Brackbill et al. [10]; k is the turbulence kinetic energy (m^2·s^{-2}); ω is the turbulence eddy frequency (s^{-1}); σ_{k3} is the Prandtl number for turbulence kinetic energy; $\sigma_{\omega 2}$ is the Prandtl number for turbulence eddy frequency in the transformed k-ε turbulence model; $\sigma_{\omega 3}$ is the Prandtl number for turbulence eddy frequency; P_k is the turbulent kinetic energy generation rate (W·m^{-3}); N_p is the number of fluid phases; F_1 is the mixing function; α_3, β' and β_3 are the turbulence model constants; r is the volume fraction and subscripts α and β are the fluid phase identification indices.

2.3. Numerical Solution Method

The aforementioned governing equations together with the initial and boundary conditions defined in Table 1 are solved numerically by using commercial CFD package ANSYS CFX [8]. Second order backward Euler method is used for integration on the transient terms with a typical time step of 1×10^{-5} s. A combination of first-order and second-order discretization schemes is applied to the spatial discretization of convective terms in the governing partial differential equations.

3. Cold Physical Model Simulation Experiments

3.1. Experimental Apparatus

In this research, in order to verify the similarity between the process of a single molten slag ligament breakup into droplets at high temperature, driven by centrifugal and surface tension forces, and that of a single water or liquid paraffin ligament disintegration into droplets at low temperature, driven by gravity and surface tension forces, and to explore the underlying theory related to the Rayleigh Disintegration Mechanism, a cold physical model experimental apparatus was set up in laboratory, as schematically shown in Figure 3, which is mainly comprised of a pressurized compartment with a pressure gauge, a capillary nozzle, a high-speed video camera and a reservoir container for receiving discharged liquid. A stopper rod was used for opening or closing the supply of the liquid and the velocity (or flowrate) of the liquid exiting the capillary nozzle forming a ligament was controlled by adjusting the pressure in the sealed compartment filled with nitrogen.

3.2. Experimental Method

As depicted by Figure 3, a container in the sealed compartment was filled with the working liquid (water or liquid paraffin) for simulating molten blast furnace slag. During the experiment, pressurized nitrogen gas was delivered into the sealed compartment. The velocity of the working liquid inside the capillary was regulated by adjusting the pressure

of nitrogen, which causes the working fluid to flow out through the capillary nozzle at the bottom to form a liquid ligament. A high-speed camera was used to capture the process of the liquid ligament breakup into droplets. During the experiment, an iron wire with known diameter was used as a reference for measuring the droplet diameter.

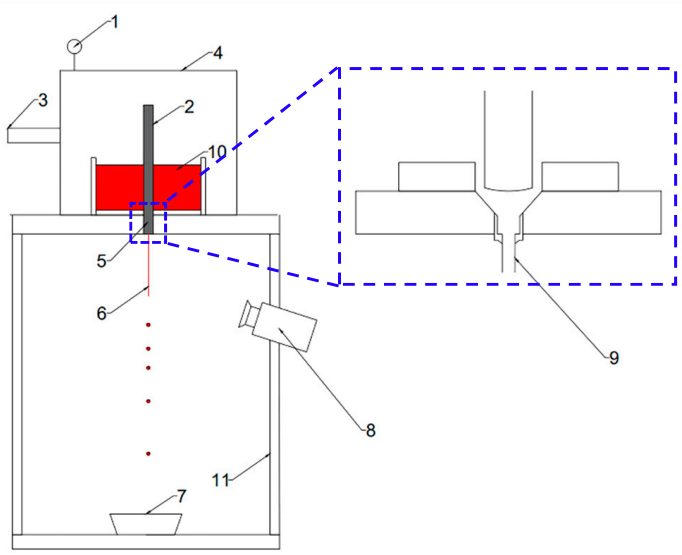

Figure 3. Schematic diagram of cold physical model experimental apparatus. 1—Pressure gauge; 2—Stopper rod; 3—Nitrogen inlet; 4—Sealed compartment; 5—Discharge nozzle assembly; 6—Liquid ligament; 7—Reservoir container; 8—High-speed video camera; 9—Capillary nozzle; 10—Water or liquid paraffin; 11—Support framework.

The influence of the liquid ligament velocity on the droplet diameter was examined in the cold physical model simulation experiments. The velocity of the liquid flowing out of the capillary nozzle was obtained from a continuity equation as follows:

$$u = \frac{V}{At} \tag{7}$$

where u is the ligament velocity at the capillary nozzle outlet (m s^{-1}); V is the measured volume of liquid flowing out of the capillary nozzle in time t (m^3); A is the capillary nozzle inner cross-sectional area (m^2) and t is the time used for the measured volume (V) of the liquid flowing out of the capillary nozzle (s).

4. Results and Discussion

4.1. CFD Model Validity

Figure 4 displays images of water droplets captured by the high-speed camera during the experiments, in which the capillary nozzle inner diameter was 1.0 mm and the velocity of water exiting the capillary nozzle, termed as ligament velocity, was controlled at 0.885 m s^{-1}, 1.089 m s^{-1} and 1.274 m s^{-1}, respectively. The average diameters of the water droplets generated under these three ligament velocity conditions were measured by means of image analysis on the recorded pictures, such as those in Figure 4. These data were used for verification of the CFD model. Figure 5 depicts a method of determining the average droplet diameter from the CFD simulation results. Taking the droplets formed at time = 0.110 s, for example, six nearly spherical shaped droplets were selected and numbered and their diameters were measured separately according to the ruler scale in the figure. The measured diameter of each droplet was given in the inset table and the average diameter of the droplets was calculated to be 2.05 mm in this example. In this way, the average diameters of the droplets were determined from all the CFD simulation cases.

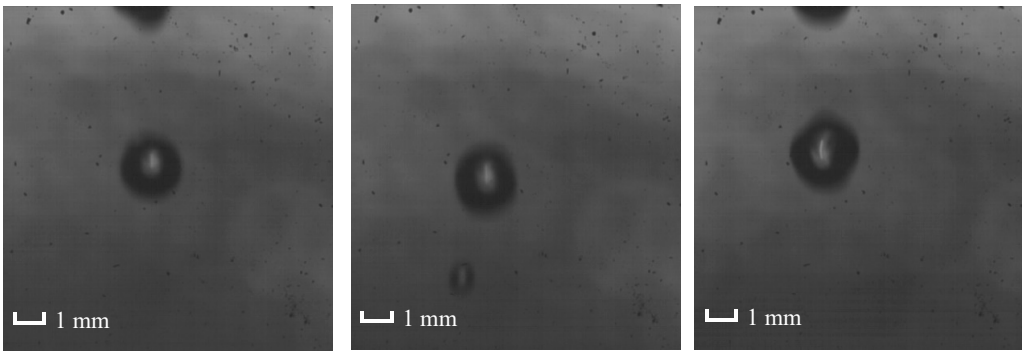

Figure 4. Images of droplets recorded with a high-speed camera at different water ligament velocities for the same apparent ligament diameter of 1 mm. (**a**) Ligament velocity: 0.885 m·s^{-1} (**b**) Ligament velocity: 1.089 m·s^{-1} (**c**) Ligament velocity: 1.274 m·s^{-1}.

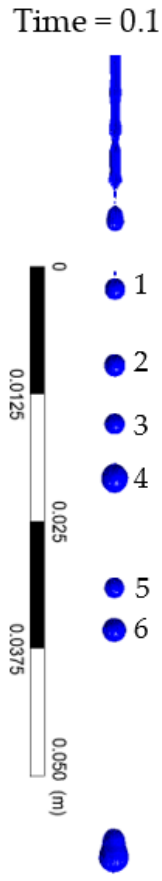

Droplet No.	Diameter (mm)
1	1.95
2	2.03
3	1.86
4	2.39
5	1.86
6	2.20
Average	**2.05**

Figure 5. Determination of average droplet diameter from CFD simulation results.

In order to validate the CFD model, the model-predicted average droplet diameter (d_p), normalized by the ligament diameter (d_l), were compared with those obtained from the water model experiments, as shown in Figure 6. It can be seen from this figure that both the CFD-model-predicted droplet size and the water-model-measured droplet size share the same variation trend with the ligament velocity, and their values are quite close to each other. The CFD model generally gives slight overestimations on the droplet size (with a maximum relative error being about 6.5%). The major cause for the error is that, in the experiments, the real ligament diameter was actually slightly smaller than the capillary nozzle inner diameter (1 mm), termed the apparent ligament diameter, while the CFD model used the exact ligament diameter (1 mm). That is why the CFD model

predicted slightly larger droplets than those measured in the experiments. According to the above error analysis, the validity of the CFD model developed in the present study can be considered acceptable.

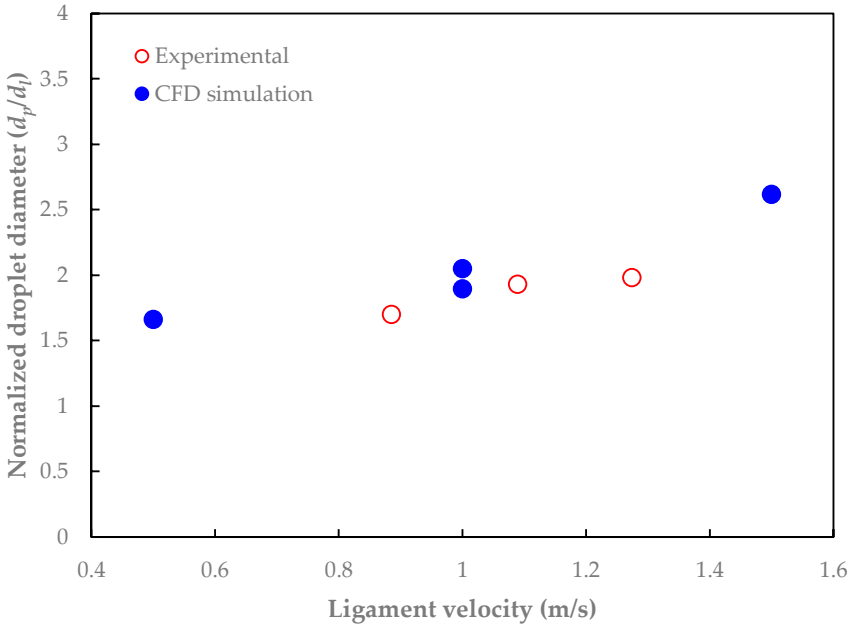

Figure 6. Comparison of normalized droplet diameter (d_p/d_l), as a function of ligament velocity, predicted by CFD model with that measured from water model.

4.2. Analyses on Numerical Simulation Results

4.2.1. Process of a Water Ligament Breakup into Droplets

Figure 7 depicts CFD-model-predicted breakup process of a water ligament exiting from a capillary nozzle of 1 mm diameter and at a velocity of 1 m s^{-1}. This figure shows that as the water flows out of the capillary nozzle, it is continually accelerated by gravity on the basis of its exit velocity (i.e., ligament velocity), and surface waves are generated in a very brief period (Figure 7a). As time proceeds, the water ligament continuously stretches, causing the droplets to develop (Figure 7b), which generally look larger than the diameter of the ligament. The ligament length (before its breakup into droplets) reaches its maximum at around 89 milliseconds (Figure 7c), after which it fluctuates within a limited range. As the unstable waves on the liquid ligament surface continuously develop, the diameter of the liquid ligament becomes increasingly uneven in the vertical direction, resulting in a number of "necks" with reduced diameters of the ligament cross-sections (Figure 7d,e). When the amplitude of the waves grows to a certain extent, the "neck" contracts to a minimum diameter so that the ligament ultimately disintegrates into droplets. Just after the droplet is separated from the ligament tip, the remaining liquid at the bottom end of the liquid ligament travels upward as a result of the imbalanced force brought on by the surface tension, which causes the ligament length to fluctuate slightly. Then, the liquid ligament disintegration repeats the aforementioned process.

According to CFD-model-simulated liquid volume fraction contour images, the average diameter of the droplets produced from a water ligament and the average length of the ligament were measured using the image analysis technique. Because the initially formed droplets were still in dynamic state and thus their shape was ellipsoidal, the lengths of each droplet's long and short axes were measured through the image analysis, and the arithmetic mean of the two was used as the diameter of the droplet.

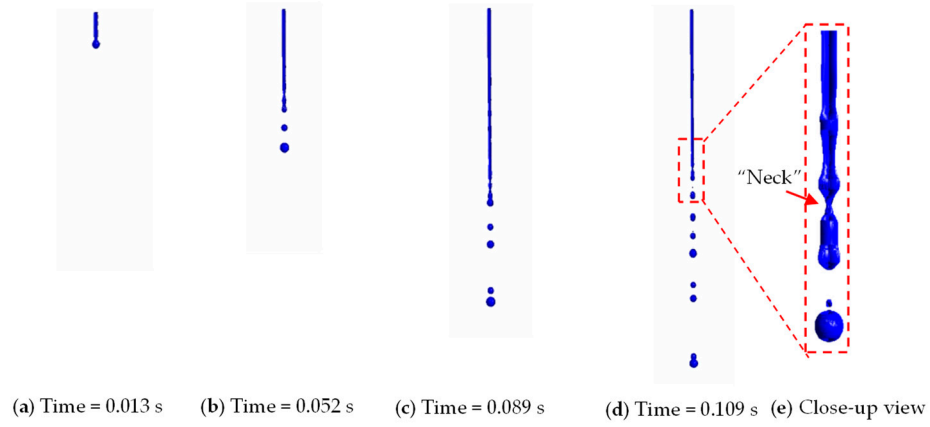

Figure 7. CFD-model-predicted process of a water ligament breakup into droplets.

4.2.2. Influence of Water Ligament Velocity on Ligament Length

Figure 8 shows the influence of the inlet velocity of water entering the computation domain, defined as ligament velocity, on the average length of the ligament. As seen from the figure, the ligament length increases with the increase of the ligament velocity. This is mainly due to the action of the inertial force, which is proportional to the flow velocity. The larger the ligament velocity, the stronger the downward inertial force and thus the longer the ligament before its breakup into droplets. Only at a certain position downstream of the water flow in the ligament, where inertial and gravitational forces are balanced by viscous and surface tension forces, does a surface wave start to form that eventually causes the breakup of the ligament into droplets. Therefore, large ligament velocity delays such surface wave formation and accordingly prolongs the ligament length.

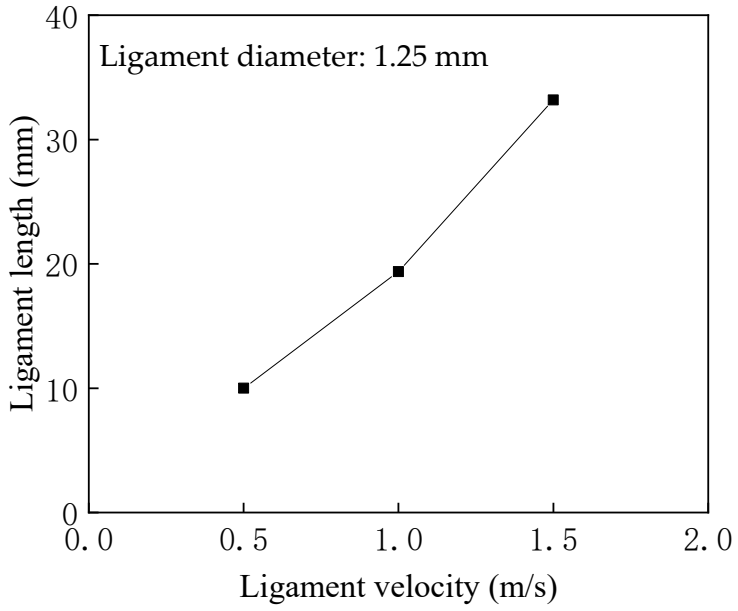

Figure 8. Influence of water ligament velocity on average length of ligament.

4.2.3. Influence of Water Ligament Velocity on Droplet Diameter

Figure 9 illustrates the effect of ligament velocity on the average diameter of droplets produced by a water ligament initially with a diameter of 1.25 mm. As seen from this figure, an increase of the ligament velocity produces larger droplets. This is due to the fact that, as the ligament velocity increases, the ligament stretches, causing the length of the surface wave to become longer; at the same time, each wave length segment gathers liquid

more quickly and more liquid accumulates in the wave length segment before the ligament "neck" breaks. As a result, larger droplets are produced at higher ligament velocity.

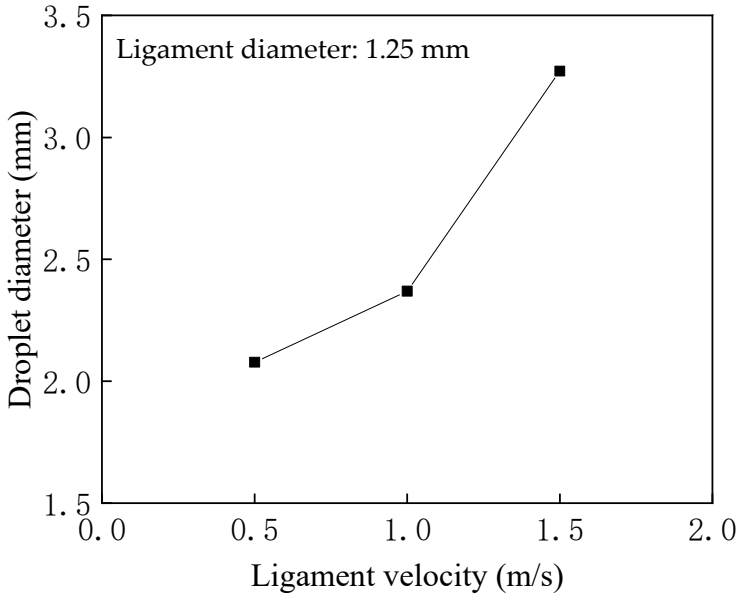

Figure 9. Influence of water ligament velocity on average diameter of droplets.

4.3. Analyses on Physical Model Experimental Simulation Results

Table 3 lists 10 sets of measurement data of water droplet diameters obtained from the cold physical model experiments on the breakup process of a water ligament exiting at different velocities from a 1 mm diameter capillary nozzle. These data reflect that the droplet diameter fluctuates within a certain range for the same ligament velocity and the fluctuation range varies with different ligament velocities. As the ligament velocity rises, the average droplet diameter increases and its fluctuation range narrows. For instance, at a ligament velocity of 0.885 m s^{-1} the average droplet diameter is 1.70 mm; the average droplet diameter increases to 1.93 mm at a ligament velocity of 1.089 m s^{-1} and, when the ligament velocity increases further to 1.274 m s^{-1}, the average droplet diameter reaches 1.98 mm.

Table 3. Water droplet diameters measured from cold physical model experiments.

Droplet Diameter (mm)	Ligament Velocity (m s^{-1})		
	0.885	**1.089**	**1.274**
D1	1.83	1.97	1.97
D2	1.74	1.95	2.00
D3	1.56	1.91	1.98
D4	1.71	1.97	1.98
D5	1.67	1.97	1.98
D6	1.68	1.89	1.98
D7	1.70	1.95	2.00
D8	1.67	1.96	1.98
D9	1.69	1.89	1.98
D10	1.70	1.86	1.97
Average	1.70	1.93	1.98

Note: Apparent ligament diameter (i.e., capillary nozzle inner diameter): 1 mm.

In addition, on the same cold physical model set-up, the authors also performed experiments on a liquid paraffin breakup into droplets. Liquid paraffin has a higher viscosity than water and is more suitable for simulating molten slag. The measured liquid paraffin droplet diameter and its apparent ligament diameter together with their ratio are given in Table 4. For the purpose of comparison, Table 4 also includes the ratio of water

droplet diameter to its apparent ligament diameter. It can be seen from this table that, on average, the diameters of liquid paraffin droplets and water droplets are approximately 1.90 and 1.86 times the diameters of their corresponding ligaments, which can be expressed by the following equations, respectively:

$$d_p \approx 1.90 d_l \tag{8}$$

for liquid paraffin ligament disintegration, and

$$d_p \approx 1.86 d_l \tag{9}$$

for water ligament disintegration, where d_p stands for droplet diameter (mm) and d_l for ligament diameter (mm).

Table 4. Droplet diameter and apparent ligament diameter and their ratio obtained from cold physical model simulation experiments.

Working Medium	Apparent Ligament Diameter d_l (mm)	Droplet Diameter d_p (mm)	d_p/d_l
Liquid paraffin	0.45	1.13	2.51
	0.60	1.25	2.08
	0.85	1.60	1.88
	1.00	1.73	1.73
	1.25	2.05	1.64
	1.45	2.25	1.55
Average			1.90
Water	1.00	1.70	1.70
	1.00	1.90	1.90
	1.00	1.98	1.98
Average			1.86

In theory, the breakup of an inviscid liquid ligament into droplets driven purely by surface tension force is described by the Rayleigh Disintegration Mechanism [7], based on which the relationship between the droplet diameter and the liquid ligament diameter can be expressed by Equation (10).

$$d_p \approx 1.89 d_l \tag{10}$$

Comparisons of Equations (8) and (9) with Equation (10) demonstrate that the disintegration processes of liquid paraffin and water ligaments under the influences of gravity and surface tension approximately follow the Rayleigh Disintegration Mechanism.

It should be emphasized here that the Rayleigh Disintegration Mechanism refers to the disintegration of a non-viscous cylindrical or ligamentous liquid into a series of identically sized droplets purely due to the effect of surface tension when the axisymmetric surface disturbance wave develops to a particular extent [7]. One of the mathematical representations of this theory is Equation (10). Influences of additional forces, such as gravity, viscous force and inertial force are mainly responsible for the discrepancy between Equations (8)–(10). Because liquid viscosity is dependent on the liquid itself, maintaining suitable ligament diameter and velocity is essential to ensuring that the ligament disintegration process closely follows the Rayleigh Disintegration Mechanism to produce uniformly sized droplets.

4.4. Comparison of Single Water Ligament Disintegration Process with Ligament Mode Breakup Process of Centrifugal Granulation of Molten Slag

By means of CFD modeling, the authors also simulated the process of the centrifugal granulation of molten slag with a spinning cup, in which the slag breaks into droplets in ligament disintegration mode [11]. Details of the modeling results are to be published. Nevertheless, some of the modeling results are presented here to demonstrate the similarity between water ligament breakup under gravity and surface tension force and molten

slag ligament breakup driven by centrifugal force and surface tension force, as shown in Figure 10. Figure 10a depicts the CFD-model-simulated process of the centrifugal granulation of molten slag operated in a regime of ligament disintegration mode, in which a number of liquid slag ligaments are formed along the circumference of the spinning cup. Focusing on the single liquid slag ligament shown in Figure 10b, under the action of centrifugal force, the ligament is continually lengthened to a certain extent at which the surface tension force creates surface waves that are evidenced by exhibiting several "necks" in the ligament, as indicated by the red arrows in the figure. Because the surface waves are unstable, further stretching of the ligament amplifies the surface wave, causing the "necks" to break and producing liquid slag droplets. Therefore, a comparison between Figure 10b,c indicates that the disintegration behavior of a curved liquid slag ligament driven by centrifugal force and surface tension is essentially similar to that of a straight water ligament driven by gravity and surface tension.

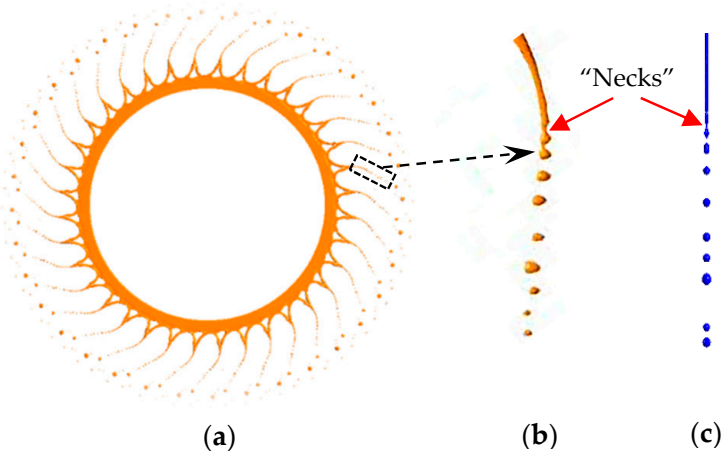

Figure 10. Comparison of disintegration process of water ligament with that of liquid slag ligament produced by spinning cup centrifugal granulation of molten slag. (**a**) CFD-model-simulated process of spinning cup centrifugal granulation of molten slag; (**b**) Close up view of disintegration process of a single slag ligament driven by centrifugal force and surface tension; (**c**) CFD-model-simulated disintegration process of single water ligament driven by gravity and surface tension.

When comparing the granulation processes of a single liquid ligament of molten slag under the influence of centrifugal force and surface tension with a single water ligament under the influence of gravity and surface tension, it is discovered that both initially create unstable disturbance waves on the surface of the liquid ligaments, causing the liquid ligament to generate a number of "necks". As the amplitude of the surface wave keeps growing, the "necks" of the liquid ligament continually contract and eventually break to form droplets.

As mentioned earlier, the breakup process of a water ligament is known to approximately follow the Rayleigh Disintegration Mechanism, and the granulation process of a liquid slag ligament is highly comparable to that of the water liquid ligament. To demonstrate this, Figure 11 shows the CFD-model-predicted average droplet diameter as a function of ligament diameter with their ratios (d_p/d_l) being marked above each data column. As the cup spinning speed has a major influence on the ligament diameter, its values corresponding to different ligament diameters are also marked in the figure. It can be seen from Figure 11 that the droplet diameter is generally proportional to the ligament diameter, both of which are influenced by the cup spinning speed. More importantly, the ratios between the droplet diameter and the ligament diameter (d_p/d_l) for different cup spinning speeds are essentially the same, and their average value is 1.84, which is well close to the value of 1.89 derived from the Rayleigh Disintegration Mechanism. Therefore, it could be said that the centrifugal granulation of molten slag in ligament disintegration

mode also approximately follows the Rayleigh Disintegration Mechanism. In this regard, we can utilize the theory of the Rayleigh Disintegration Mechanism to guide the design and operation of the centrifugal granulation of molten slag using a spinning cup. That is, to find appropriate design and operating parameters to produce liquid slag ligaments at the cup edge with suitable properties (ligament diameter and velocity, both dependent on the spinning cup's diameter, spinning speed and slag flowrate), so that the diameter of the droplets formed from disintegration of such slag ligaments can be approximately in accordance with the law outlined by Equation (10), so as to produce uniform slag particles with controllable size.

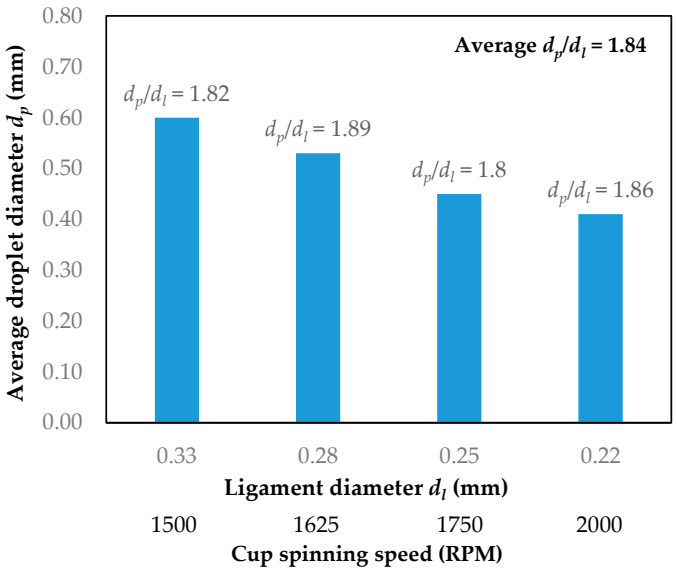

Figure 11. CFD-model-predicted average droplet diameter as a function of ligament diameter in the process of centrifugal granulation of molten slag with a spinning cup.

5. Conclusions

In the present work, the processes of single water and liquid paraffin ligament breakup into droplets driven by gravity and surface tension force were investigated through performing cold physical model experiments and CFD numerical simulations. The aim of the work was to study the similar process of liquid slag ligament breakup into droplets during the centrifugal granulation of molten slag using a spinning cup. Influences of liquid ligament velocity and diameter on droplet diameter were specially examined. The following conclusions can be drawn:

(1) The CFD model simulation results on a single water ligament breakup demonstrate that a larger liquid ligament velocity leads to a longer ligament that eventually breaks into larger droplets. When the velocity of a 1 mm diameter water ligament increases from 0.5 m s^{-1} to 1.0 m s^{-1}, the average ligament length and average droplet diameter increase by 9.38 mm and 0.291 mm, respectively.

(2) The cold physical model experimental results indicate that the disintegration processes of water and liquid paraffin ligaments driven by gravity and surface tension force closely follow the Rayleigh Disintegration Mechanism. The average ratios between the droplet diameter and the ligament diameter for water and liquid paraffin are around 1.86 and 1.90, respectively, which well approach the theoretical ratio of 1.89 derived from the Rayleigh Disintegration Mechanism.

(3) CFD simulation results on the process of the centrifugal granulation of molten slag using a spinning cup demonstrate that the breakup process of liquid slag ligaments formed at the cup circumference exhibits similar characteristics to that of water and liquid paraffin ligament breakup, which also approximately follow the Rayleigh Disintegration Mechanism. Therefore, this theory can be utilized to guide the design and operation of

spinning cup centrifugal granulation of molten slag in ligament disintegration mode, so as to produce uniform slag particles with controllable size.

Author Contributions: Conceptualization, M.Z. and Y.P.; methodology, A.Z. and S.Z.; validation, M.Z. and A.Z.; formal analysis, M.Z., Y.P. and A.Z.; investigation, M.Z., A.Z. and S.Z.; resources, P.M. and X.F.; data curation, M.Z. and A.Z.; writing—original draft preparation, M.Z., A.Z. and S.Z.; writing—review and editing, Y.P. and P.M.; visualization, A.Z. and S.Z.; supervision, Y.P. All authors have read and agreed to the published version of the manuscript.

Funding: This research received no external funding.

Data Availability Statement: Not applicable.

Acknowledgments: The authors would like to thank the University of Science and Technology Liaoning for financial support for the present research work.

Conflicts of Interest: The authors declare no conflict of interest.

References

1. McDonald, I.; Werner, A. Dry slag granulation–the environmentally friendly way to making cement. In Proceedings of the Aisa Steel International Conference, Beijing, China, 1 January 2012.
2. Wang, J.; An, B.; Liu, J. On the sensible heat recovery technique by granulating blast furnace slag with rotary cup. *Energy Energy Conserv.* **2014**, *6*, 129–132. (In Chinese)
3. Yu, P.; Wang, S. Current and future of dry centrifugal granulation process. *Key Eng. Mater.* **2016**, *719*, 92–97. [CrossRef]
4. Gao, J.; Feng, Y.; Zhang, W.; Feng, D.; Zhang, X. Prediction on particle size characteristics of high-temperature liquid blast furnace slag in a centrifugal granulation process. *Powder Technol.* **2020**, *376*, 527–536. [CrossRef]
5. Dombrowski, N.; Lloyd, T. Atomisation of liquids by spinning cups. *The Chem. Eng. J.* **1974**, *8*, 63–81. [CrossRef]
6. Wegener, M.; Muhmood, L.; Sun, S.; Deev, A.V. The formation and breakup of molten oxide jets. *Chem. Eng. Sci.* **2014**, *105*, 143–154. [CrossRef]
7. Lord Rayleigh, F.R.S. On the instability of jets. *Proc. Lond. Math. Soc.* **1878**, *10*, 4–13. [CrossRef]
8. ANSYS Inc. *ANSYS CFX User's Manual, Release 18.0*; ANSYS Inc.: Canonsburg, PA, USA, 2017.
9. Hirt, C.W.; Nichols, B.D. Volume of Fluid (VOF) method for the dynamics of free boundaries. *J. Comput. Phys.* **1981**, *39*, 201–225. [CrossRef]
10. Brackbill, J.U.; Kothe, D.B.; Zemach, C. A continuum method for modeling surface tension. *J. Comput. Phys.* **1992**, *100*, 335–354. [CrossRef]
11. Hinze, J.O.; Milborn, H. Atomization of liquids by means of a rotating cup. *J. Appl. Mech.* **1950**, *17*, 145–153. [CrossRef]